Surface modification of beidellite – a TG, FTIR and SEM study

Yet Hong Lim, Emily Grundgeiger, Sara Couperthwaite, Ray L. Frost, Godwin A. Ayoko and Yunfei Xi *

Nanotechnology and Molecular Science Discipline, Faculty of Science and Engineering, Queensland University of Technology, 2 George Street, Brisbane, QLD 4000, Australia.

Abstract:

Natural beidellite was modified with a cationic surfactant - octadecyltrimethylammonium bromide at different concentrations. Changes on the surface and structure of beidellite were recorded by a series of characterisation methods. Thermogravimetric analysis was used for probing the different surfactant molecule environments based on different decomposition temperatures; confirmations of intercalated surfactants were revealed by combining thermogravimetric analysis and Fourier transform infrared spectroscopy results. Morphologies of the modified beidellites were investigated by Scanning Electron Microscopy. It was observed that the physical and chemical properties of the beidellite changed significantly upon surfactant modification.

Keywords: beidellite; organo-beidellite; octadecyltrimethylammonium bromide; TG; FTIR; SEM.

* Corresponding author, Tel: +61 7 3138 1466

E-mail address: y.xi@qut.edu.au

1. Introduction

The smectite group of clay minerals represents the most important phyllosilicates which are widely used in a range of applications because of their cation exchange capacities, high surface areas and resulting high adsorption capacities. Organic surfactant modified clays (organo-clays) are well known adsorbents due to their superior adsorption property, abundance, porosity, high surface area and relatively low cost [1]. Recent studies indicate that numerous applications in environmental remediation have fully utilised the properties of organo-clays [2-5].

Though both montmorillonite (denoted as Mt) and beidellite (denoted as Bd) belong to the smectite group [6], Mt is one of the most studied clay minerals. There are numerous publications on the properties of organic surfactants modified Mt [7-14]. However, the property and the potential application of Bd have received less attention [15]. In common with Mt, Bd consists of 2:1 TOT layers with an ideal formula $(Al_{4.00})(Si_{7.15}Al_{0.85})_{20}(OH)_4X_{0.85}nH_2O$ [16]. The net negative surface charge on Bd usually originates from the isomorphous substitution of Al^{3+} for Si^{4+} in the silicate tetrahedral sheets [16], while the charge of Mt is from the octahedral substitution of Al^{3+} by Mg^{2+}. Inorganic cations such as Na^+ and Ca^{2+} are attracted to the negatively charged layers. Bd can be organically modified and used for environmental contaminants remediation . The properties of Bd, for example, its swelling property, surface area and adsorption property, are enhanced by intercalating cationic organic surfactants [17].

To the best of our knowledge, compared to Mt, there are fewer studies on Bd/organo-Bd, particularly on their characterisations. In this study, Bd was modified with a long chain cationic surfactant, octadecyltrimethylammonium bromide (denoted as ODTMA). The prepared organo-Bd (denoted as OBd) were characterised by thermogravimetric (TG) analysis and Fourier transform infrared (FTIR). The morphologies of unmodified/modified

Bd were studied using scanning electron microscope (SEM). The changes in the structure and morphology of OBd prepared using various surfactant concentrations were investigated and discussed.

2. Materials and methods

2.1. Chemicals

The SBId-1 Bd, obtained from Clay Minerals Repository USA, has a cation exchange capacity (CEC) of 129 meq / 100 g [18]. ODTMA ($C_{21}H_{46}NBr$, MW: 392.5) was obtained from Sigma-Aldrich and its molecular structure is illustrated in Fig. 1. All materials were used as received without purification.

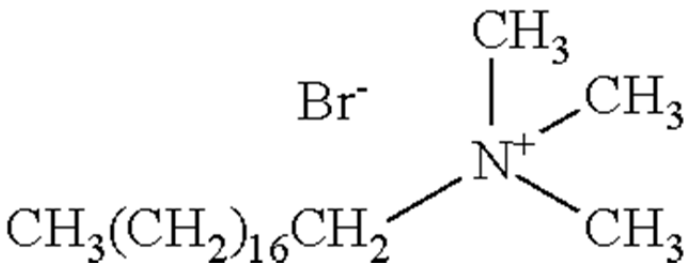

Figure 1: Molecular structure of ODTMA.

2.2. OBd preparation

Synthesis of OBd was undertaken by the following procedure: Bd was finely grounded using an agate mortar then sieved through a 250 μm sieve. 4 g of Bd was dispersed into 400 mL of Purelab Flex deionised water. The clay suspension was stirred at 600 rpm for 1 h using a magnetic stirrer. Stoichiometric amount of 25% (0.25 CEC), 50% (0.50 CEC), 100% (1.00 CEC) and 200% (2.00 CEC) of ODTMA was slowly added into the clay suspension and stirred at 600 rpm at room temperature for another 3 h. The mixture was allowed to settle overnight and the supernatant was decanted. OBd were recovered by a

centrifuge and washed with Purelab Flex deionized water until free of bromide anions as determined by $AgNO_3$ test. All samples were dried at room temperature and stored in plastic sample containers in a vacuum desiccator. The prepared OBd, with surfactant loadings corresponding to 0.25 to 2.00 CEC, were denoted as 0.25CEC-OBd, 0.5CEC-OBd, 1.00CEC-OBd and 2.00CEC-OBd, respectively. The unmodified beidellite was denoted as Bd.

2.3. Sample characterisation

Thermogravimetric analyses of the Bd, OBd and ODTMA were performed using a TA Instruments Inc. Q500 high-resolution TGA operating at a ramp of 5.0˚C/min with 6.0˚C resolution from room temperature to 1000˚C in a high purity flowing nitrogen atmosphere (60 mL/min). Each analysis was obtained with approximately 40-50 mg of finely ground sample heated in an open platinum crucible.

Infrared (IR) spectra were obtained using a Nicolet Nexus 870 FTIR spectrometer equipped with a diamond ATR accessory. Spectra over the 4000–550 cm^{-1} range were obtained by the co-addition of 64 scans with a resolution of 4 cm^{-1} and a mirror velocity of 0.6329 cm/s. Band component analyses were undertaken using the 'Peakfit' software package. This software enabled the type of fitting function to be selected and allows specific parameters to be fixed or varied accordingly. Band fitting was done using a Lorenz–Gauss cross-product function with the minimum number of component bands used for the fitting process.

A FEI Quanta 200 scanning electron microscope (SEM) with integrated energy dispersive X-ray analyser (EDX) system was used for morphological studies. All samples were dried at room temperature and coated with gold for the SEM studies.

3. Results and discussion

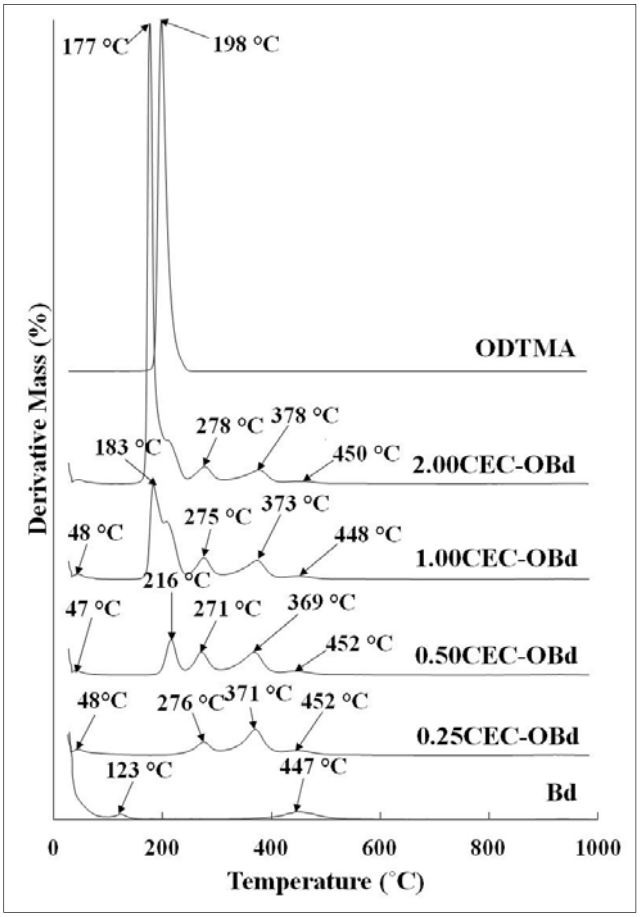

Figure 2: DTG patterns of Bd, OBd and ODTMA.

Thermogravimetric analysis can provide an insight of the thermal stability and packing arrangement of the surfactant molecules within OBd. The differential thermogravimetric – DTG (derivative wt% versus temperature) plots are illustrated in Fig. 2. Generally, there are several mass loss steps that are observed for each sample.

There are three decomposition steps in Bd. The first step with about 8% mass loss is from the loss of physical adsorbed water. Compared to the mass loss of physical adsorbed water in OBd, Bd contains more water. The second mass loss (~1.2%) occurring at about 123°C is contributed to the dehydration of water molecules around exchangeable metal cations such as Na^{+} or Ca^{2+} [19]. The third mass loss (53%) peaked at around 447˚C is

assigned to the loss of structural OH units of the clay [19]. It is observed that the dehydration of water molecules on exchangeable sites appear only in Bd which suggests that in OBd most of the water molecules have been replaced by cationic surfactant ions. The position of desurfactant (decomposition of surfactant) temperature in the curves of the OBd is confirmed by comparison with the DTG curve of the pure ODTMA which shows a single intense peak at 198˚C [20]. Similar to previous studies, more than one peak for desurfactant processes can be observed which indicate that the surfactant molecules present in different environments within organo-clays [20, 21].

For 0.25CEC-OBd, two desurfactant steps are observed. The decomposition of intercalated surfactant occurs at 371°C with a mass loss of 8.32%. A mass loss of 3.63% at 276°C is due to ODTMA present internally, but only weakly held there by intermolecular attractions between the long alkyl chains of the surfactant. Dehydroxylation occurs at 452°C with a mass loss of 2.33 %.

In contrast, 0.5CEC-OBd, 1.0CEC-OBd and 2.0CEC-OBd show three distinct peaks for the desurfactant processes. The surfactant on the surface of the clay is least thermally stable and is the first to be decomposed. The next mass loss of surfactant is due to ODTMA molecules which present internally as discussed above. The third mass loss in the desurfactant process, is from the exchanged ODTMA actually adsorbed on the internal exchangeable sites of the clay which has the highest decomposition temperature. Compared with the decomposition temperature of pure ODTMA surfactant at 198˚C, it is observed that the surfactant molecules on the internal exchangeable sites of OBd are more thermal stable and the central peak position shifts slightly from 371˚C of 0.25CEC-OBd, 369˚C of 0.50CEC-OBd, 373˚C of 1.00CEC-OBd to 378˚C of 2.00CEC-OBd. With the increase of surfactant loading from 50% to 200% CEC, the intensity of the first desurfactant peak increases and the temperature decreases from 216°C (0.50 CEC) to 177°C (2.00 CEC). The

intensity of the second peak remains almost unchanged, but the temperature increases from 271°C (0.50 CEC) to 278°C (2.00 CEC).

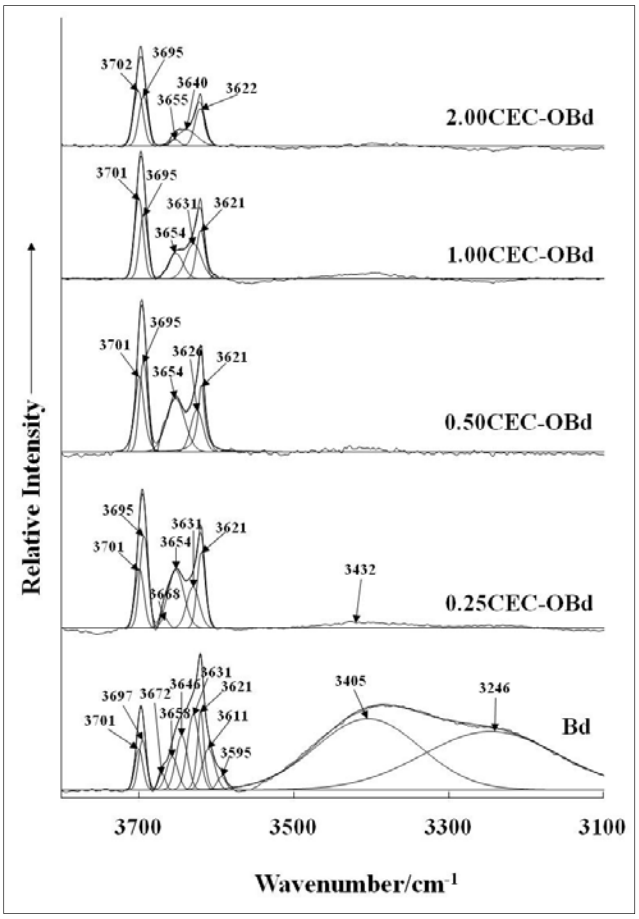

Figure 3: FTIR spectra (3800-3100 cm^{-1}) of Bd and OBd.

Fig. 3 shows the infrared spectra of Bd and OBd at 3800 – 3100 cm^{-1} region. Bd shows two broad OH stretching bands at 3405 cm^{-1} and 3246 cm^{-1}, respectively, which are attributed to water molecules absorbed within the interlayer of the clay [19, 22]. In contrast, no noticeable peak can be observed at this region for OBd. Sharp peaks observed at region 3500 cm^{-1} – 3700 cm^{-1} are assigned to the OH vibration of the structural hydroxyl group. In Bd, two bands are observed at 3701 cm^{-1} and 3697 cm^{-1}, respectively and these OH vibration bands are relatively independent to the surfactant concentration.

For 0.25CEC-OBd, the band at 3654 cm^{-1} with a shoulder at 3668 cm^{-1} and the band at 3631 cm^{-1}, are dependent on the concentration of the loaded surfactant. It can be observed that the wavenumbers of the band increases slightly (3654 cm^{-1} to 3655 cm^{-1}) and the intensity of the band decreases. The changes in intensities are related to the environment of the water and hence, it suggests that the water within has been replaced by surfactant molecules [19]. Similar phenomenon can also be observed for a band observed at 3621 cm^{-1}.

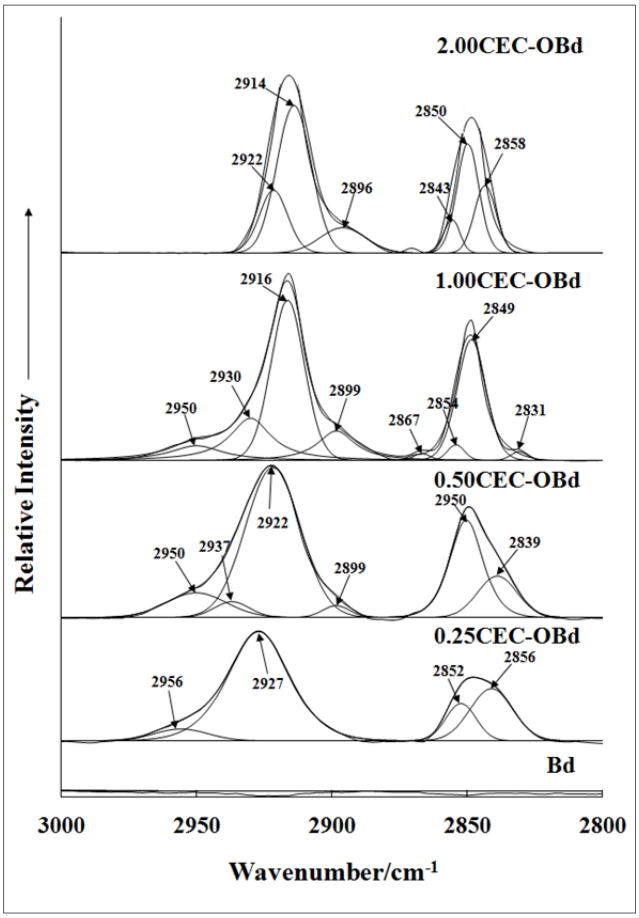

Figure 4: FTIR spectra (3000-2800 cm^{-1}) of Bd and OBd.

Fig. 4 illustrates the IR spectra of CH stretching vibration region. For Bd, no bands of symmetric and asymmetric CH_2 were observed in the spectrum. For OBd, the bands at about 2850 and 2930 cm^{-1} are assigned to the asymmetric $\nu_{as}(CH_2)$ and symmetric $\nu_s(CH_2)$

161 stretching modes of the methyl groups of the surfactant. The wavenumbers of both $\nu_s(CH_2)$
162 and $\nu_{as}(CH_2)$ stretching are very sensitive to conformational changes. The changes are
163 dependent on the concentration of the loaded surfactant. It is observed that the frequencies of
164 symmetric and asymmetric CH_2 stretching slightly shifted to lower wavenumbers with the
165 increase of surfactant loading. In the case of asymmetric CH_2 stretching, the wavenumber
166 shifts from 2927 cm^{-1} for 0.25CEC-OBd to 2914 cm^{-1} for 2.0CEC-OBd. On the other hand,
167 the wavenumber of symmetric CH_2 stretching shifted from 2852 cm^{-1} (0.25CEC-OBd) to
168 2850 cm^{-1} (2.0CEC-OBd). These changes in wavenumbers indicate conformational
169 differences in various concentrations of surfactant loaded Bd. It was reported that symmetric
170 and asymmetric CH_2 stretching modes are extremely sensitive to the conformational changes
171 [23]. The shift to a lower wavenumbers suggest a higher ordered *all-trans* conformation [24].
172 At higher packing density, the adsorbed surfactant molecules form a solid like molecular
173 environment.

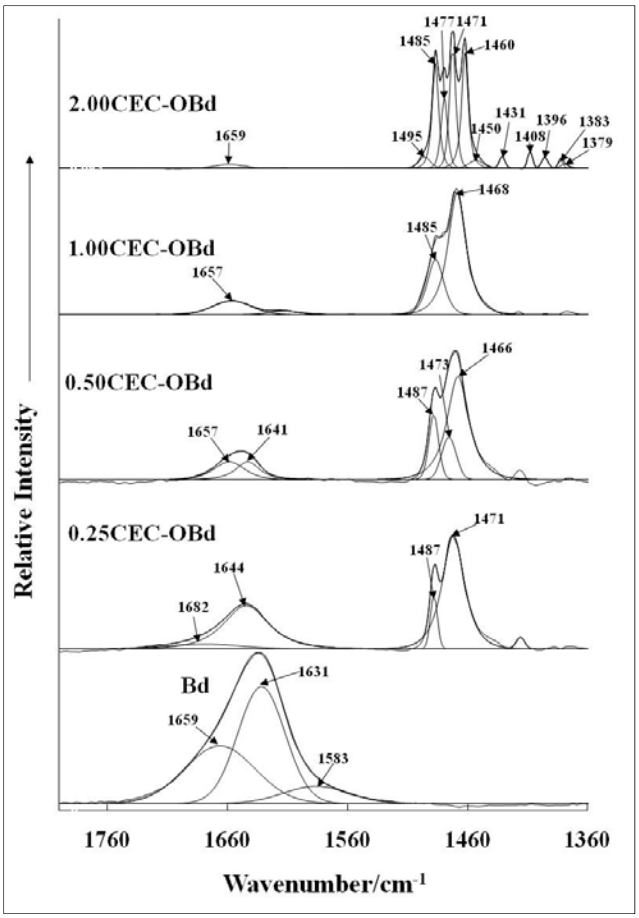

Figure 5: FTIR spectra (1800-1360 cm^{-1}) of Bd and OBd.

Water bending bands are observed in the 1800 cm^{-1} to 1500 cm^{-1} region as shown in Fig. 5. The intensity of the bands decreases as the concentration of the loaded surfactant increases which suggests that Bd contains more adsorbed water. With the increase of loaded surfactant amount, adsorbed water molecules are gradually replaced by ODTMA, which results in the decrease in intensity. The shift to higher wavenumbers is also observed with the increase of surfactant loading. Similar to CH_2 stretching region as discussed earlier in this manuscript, in Bd, no bands from HCH deformation region $\delta(CH_2)$ at around 1400 to 1500 cm^{-1} are observed [23]. With modified Bd at lower surfactant concentrations, two main peaks at about 1487 cm^{-1} and 1471 cm^{-1} are observed. Surfactant peaks which started to emerge at 1431 cm^{-1}, 1408 cm^{-1}, 1396 cm^{-1} and 1383 cm^{-1} for 2.0CEC-OBd are attributed to the

ODTMA, indicating that Bd has reached its acme point of the surfactant intake. The spectrum at this region indicates that the methyl group shows significant changes with increase in surfactant loading, and it can be concluded that due to the intercalation, the methyl group is attracted to the siloxane surface and hence, free rotation of the methyl group is no longer possible [23].

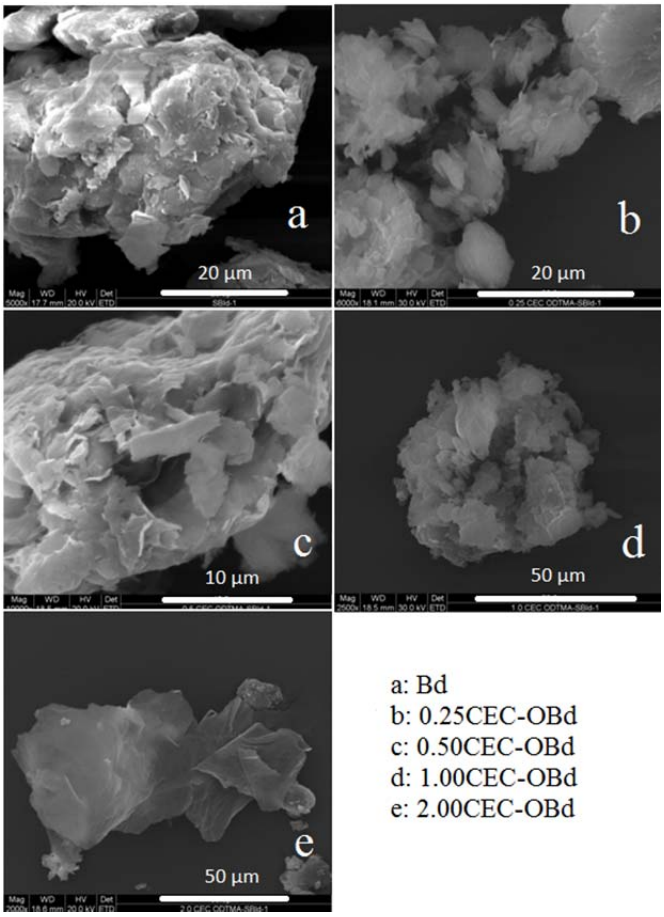

Figure 6: SEM images of Bd (a), 0.25CEC-OBd (b), 0.50CEC-OBd (c), 1.00CEC-OBd (d), and 2.00CEC-OBd (e).

Bd (Fig. 6a) shows morphology with massive and aggregated small flakes. OBd appeared to have more fragments. The fragments observed are generally smaller in size with irregular shapes. At lower concentration of surfactant loading, the Bd flakes appeared to be

more fluffy (Fig. 6b) and with the increase of surfactant loading, the Bd flakes appear to be more rigid and more layered like (Fig. 6e). At higher concentration of surfactant loadings (1.0 and 2.0 CEC, as shown in Fig. 6d and 6e, respectively), the Bd flakes appear to be flat. Generally, there are no significant morphological differences between Bd and OBd.

4. Conclusions

In this study, the OBd were synthesised using surfactant ODTMA at different concentrations. TG, FTIR and SEM have been used to characterize and compare the differences between unmodified and modified Bd at different surfactant loadings. Derivative TG has revealed that there are a few mass losses in OBd, while surfactant molecules in different environments have variable thermal stabilities. According to SEM results, there are no significant morphological differences between Bd and OBd. For unmodified and modified Bd, OH stretching, CH stretching, HOH and HCH bending vibration regions are investigated and compared using FTIR. This type of organo-clay has potential to be a promising adsorbent material for environmental organic contaminants.

Acknowledgements

The authors also thank Queensland University of Technology (QUT) for the provision of the facilities and infrastructure used for the work. In addition, YX thanks the QUT's Vice Chancellor for the award of a research grant.

References

[1] H. He, L. Ma, J. Zhu, R.L. Frost, B.K.G. Theng, F. Bergaya, Appl. Clay Sci. 100 (2014) 22.
[2] F. Bergaya, G. Lagaly, Dev. Clay Sci. 1 (2006) 1.
[3] N. Bektas, S. Aydin, M.S. Oncel, Sep. Sci. Technol. 46 (2011) 1005.
[4] L. Jiunn-Fwu, M.M. M, C.C. T, K.D. E, B.S. A, Clays and Clay Minerals 38 (1990) 113.
[5] G.W. Beall, Applied Clay Science 24 (2003) 11.
[6] F. Bergaya, G. Lagaly, K. Beneke, Dev. Clay Sci. 1 (2006) 1163.
[7] Y. Park, Z. Sun, G.A. Ayoko, R.L. Frost, Chemosphere 107 (2014) 249.

[8] Y. Park, G.A. Ayoko, E. Horvath, R. Kurdi, J. Kristof, R.L. Frost, J. Colloid Interface Sci. 393 (2013) 319.
[9] P. Wu, Y. Dai, H. Long, N. Zhu, P. Li, J. Wu, Z. Dang, Chemical Engineering Journal 191 (2012) 288.
[10] B. Liu, J. Lu, Y. Xie, B. Yang, X. Wang, R. Sun, Journal of Colloid and Interface Science 418 (2014) 311.
[11] J. Zhu, Y. Qing, T. Wang, R. Zhu, J. Wei, Q. Tao, P. Yuan, H. He, Journal of Colloid and Interface Science 360 (2011) 386.
[12] M. Ghayaza, L. Le Forestier, F. Muller, C. Tournassat, J.-M. Beny, Journal of Colloid and Interface Science 361 (2011) 238.
[13] Y. Xi, W. Martens, H. He, R.L. Frost, Journal of Thermal Analysis and Calorimetry 81 (2005) 91.
[14] Q. Zhou, R.L. Frost, H. He, Y. Xi, Journal of Colloid and Interface Science 314 (2007) 405.
[15] B. Paul, W.N. Martens, R.L. Frost, Appl. Surf. Sci. 257 (2011) 5552.
[16] A.C.D. Newman, Chemistry of clays and clay minerals. Wiley, New York, 1987.
[17] E. Grundgeiger, Y.H. Lim, R.L. Frost, G.A. Ayoko, Y. Xi, Applied Clay Science 105–106 (2015) 252.
[18] V. Aggarwal, H. Li, B.J. Teppen, Environ. Toxicol. Chem. 25 (2006) 392.
[19] Y. Park, G.A. Ayoko, R.L. Frost, Journal of Colloid and Interface Science 360 (2011) 440.
[20] Y. Park, G.A. Ayoko, R.L. Frost, J Colloid Interface Sci 360 (2011) 440.
[21] Y. Xi, R.L. Frost, H. He, J Colloid Interface Sci 305 (2007) 150.
[22] F.B.a.J.J.F. E. Srasra, Clays and Clay Minerals 42 (1994) 237.
[23] Y. Xi, Z. Ding, H. He, R.L. Frost, Spectrochimica Acta Part A: Molecular and Biomolecular Spectroscopy 61 (2005) 515.
[24] R.A. Vaia, R.K. Teukolsky, E.P. Giannelia, Chemistry of Materials 6 (1994) 1017.